

## NON-PROPORTIONAL NONLINEAR DAMPING IN EXPERIMENTAL BLADED DISK

Ladislav Půst, Luděk Pešek\*

*Paper is concerned with the flexural vibrations of imperfect bladed circular disk by analytical and numerical solutions. Disk imperfection results from additional two groups of damping heads fixed on opposite ends of one diameter, which introduces point imperfections in mass, stiffness and nonlinear damping and non-proportional distribution of damping properties. The aim of this study is to investigate influence of friction damping among added bladed heads on decrease of resonance amplitudes. Examples based on application of equivalent linearized damping show the properties of such dampers.*

*Keywords: bladed disk vibrations, dry friction damping, imperfection, non-proportionality, response curves*

### 1. Introduction

In order to quench unwanted and very dangerous vibrations of turbine bladed disks, various types of dampers are used and the large-scale research on this problem has been carried out in many institutes and laboratories in the world (e.g. [1–3]). Also in laboratories IT AVCR, the experimental model of bladed disk is investigated and applied for study of various damping principle. The presented paper is a contribution to elaboration of basic theoretical background for analysis of data gained by measurement on real structure or on experimental model of turbine disks [4, 5]. The investigated experimental dampers for reduction of undesirable blade vibrations are based on dry friction principle, which due to its strong nonlinearity cannot be solved by a usual methods of solution used for linear vibrating system [6–8].

In the first part of this paper, the spectral and modal analysis of a FE model of bladed disc stationary fixed in its center is applied for ascertaining of several lowest eigenfrequencies and compared with measurement. Analytical analysis of influence of dry friction element on the disk behaviour is carried out by means of equivalent linearization. The irregular distribution of damping heads on the disk circumference results into non-proportional damping and influences also the dynamic properties.

The possibility how suppress resonance vibrations by using the dry friction element is shown on examples.

### 2. FE model of bladed disk

Theoretical analyses of dynamic properties of experimental model consisting of a steel disk with 60 prismatic models of blades fastened on the perimeter of disk and provided with

---

\* Ing. L. Půst, DrSc., Ing. L. Pešek, CSc., Institute of Thermomechanics AS CR, v.v.i., Dolejškova 5, 182 00 Praha 8

damping heads clustered in two groups of five blades lying on opposite ends of one diameter were done both by a FE calculation of standing disk and analytically on a simplified model of rotating disk.

A three dimensional FE-model, shown in Fig. 1, has been developed and used for calculation of eigenvalues and eigenmodes of vibrations. Damping elements were fixed connected with the blade ends for modal analysis.

Due to the added masses on ends of selected blades, the bladed disk losses its perfect circular properties with infinite number of symmetry axis and become imperfect one with countable number of axis, in our case with two symmetry axes. Perfect disks have double eigenfrequencies, which split into pairs of close eigenfrequencies at imperfect disks.

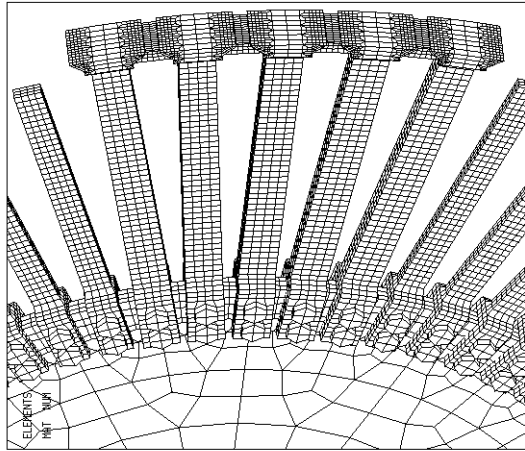


Fig.1

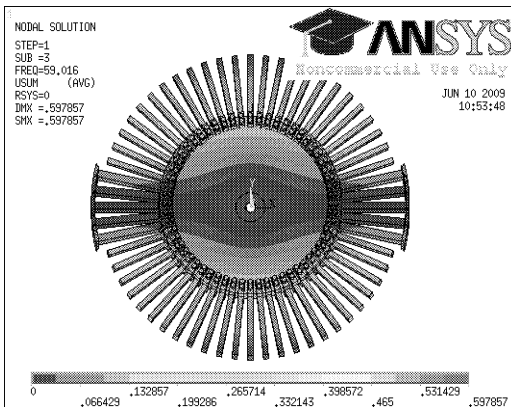


Fig.2

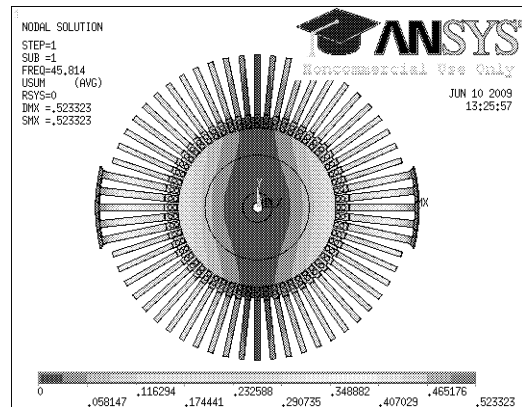


Fig.3

As result of this FE analysis are in Fig. 2 and 3 shown calculated modes of lowest pair of split eigenfrequencies  $f = 59.016\text{Hz}$  and  $f = 45.814\text{Hz}$ . One nodal diameter is identical with axis going through the added masses at higher frequency and the other symmetry axis is perpendicular to the previous one. The eigenfrequencies of three lowest modes with 1, 2 and 3 nodal diameters and with no nodal circle are given in Table 1, where the abbreviations NC=Nodal Circle and ND=Nodal Diameter are used.

FEM calculation		experiment		Mode parameters
Imperfect disk	Perfect disk	With fixed dampers		
Eigenfrequency [Hz]		Damping [%]		
45.814	59.21			ND = 1, NC = 0
59.016	59.21	54.8	0.52	
72.696	78.596	71.6	0.37	ND = 2, NC = 0
77.978	78.596	77	0.1	
107.19	121.05	102	0.22	ND = 3, NC = 0
120.94	121.06	113	0.11	

Tab.1

The calculated frequencies of imperfect disk, where the moving parts of dampers are fixed to the dampers bodies, are compared with the eigenfrequencies of perfect disk without dampers and also with the result of the first measurement on the imperfect bladed disk fixed in its center to the heavy block. This measurement data were gained by modal analysis based on impact hammer method with use of apparatus PULSE10.0 for data acquisition and MeSCOPE for global identification.

**3. Effect of imperfection**

Dampers added in a limited number of blades introduce imperfection. New dynamic properties of bladed disk, which losses its perfect circular properties, characterized by infinite number of symmetry axis, is evaluated. The damper heads on a family of five blades are realized by fixed small masses on blade ends. These heads are mutually connected by friction contacts via small friction elements, which allow only the axial relative motion between neighboring heads, but suppress their relative turning and cause an increase of bending stiffness in circumferential direction.

There are eight friction contacts between the blade heads and small friction elements pressed into the wedge-shaped gaps by a centrifugal force. Due to this very complicated nonlinear structure of cluster of damped blades it is necessary to introduce a simple model of damping heads cluster for computational purposes.

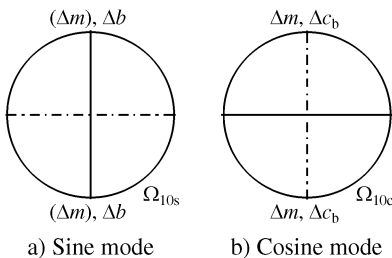


Fig.4

This model consist of added mass  $\Delta m$ , additional damping  $\Delta b$  and also additional stiffness  $\Delta c$  concentrated into one point at the ends of corresponding diameter – symmetry axis of imperfect disk.

These imperfections influence the individual orthogonal eigen-modes splitting in different way. These different influences are demonstrated on the simple split modes with one modal diameter shown in Fig. 4. When the disk vibrates by the sine mode with the node-line going through this imperfection at eigenfrequency  $\Omega_{10s}$  (Fig. 4a)

(Fig. 4a) the additional masses  $\Delta m$  do not move and therefore they have no influence on vibrations. But the shear forces between the damping heads at this mode are at sine mode the biggest, the amplitudes of neighbouring blades are very different and therefore the increase of damping influences on this sine mode is strong.

In the second split cosine mode (Fig. 4b) of the eigenfrequency  $\Omega_{10c}$  the imperfections vibrate in the antinode positions, where amplitudes of neighbouring blades are maximum

but approximately equal, the damping is minimum, but as the amplitudes and curvature in anti-node are greatest, the influence of added masses and bending circumferential stiffness are important for cosine mode.

With respect to these properties, the motion equations of imperfect disk with damping heads in the frequency range  $\omega$  near a single pair of split eigenfrequencies  $\Omega_{10s}$  and  $\Omega_{10c}$  are as follows :

$$\begin{aligned} m_{red} \ddot{q}_s + (b_{red} + 2 \Delta b) \dot{q}_s + c_{red} q_s &= K f(r) \sin \varphi F_0 \cos \omega t \sin(\lambda) , \\ (m_{red} + 2 \Delta m) \ddot{q}_c + b_{red} \dot{q}_c + (c_{red} + 2 \Delta c_b) q_c &= K f(r) \cos \varphi F_0 \cos \omega t \cos(\lambda) , \end{aligned} \tag{1}$$

where  $m_{red}$ ,  $b_{red}$ ,  $c_{red}$  are reduced values of perfect disk masses, damping and stiffness. Function  $f(r)$  denotes the form of vibrations in the radial direction.  $K f(r)$  is a function depending on the structure and mass distribution of disk vibrating with the mode of one nodal parameter and no nodal circle ( $\Omega_{10}$ ). Expression  $F_0 \cos \omega t$  is single point exciting force. Angle  $\lambda$  expresses the position of this force on the periphery of stationary disk. Variable  $q_s$ ,  $q_c$  are the normal coordinates corresponding to the split sine and cosine mode of disk vibration with one nodal diameter and no nodal circle. The equations (1) are linear, but the additional damping force  $2 \Delta b \dot{q}_s$  in the real bladed disk with friction dampers is strongly nonlinear due to the dry friction. Influence of added mass  $\Delta m$  on dynamic behaviour of disk does not change the linearity of investigated system, as well as the additional bending stiffness  $\Delta c$ , which can be explained as influence of partial shroud of five blades.

#### 4. Dry friction damping

As mentioned in previous chapter, the behaviour of friction connection between blades has strongly nonlinear characteristic and its influence on dynamic properties of bladed disk must be taken into account. Dry friction is very complicated process and the generally used Coulomb model is only the first approximation of real properties. For better description of friction process, the micro-slips at the very low velocity  $v$  has to be introduced, as well as the friction force increase or decrease at higher velocity. The micro-slips at the very low velocity  $v$  can be modelled by a linear increase of friction force, as shown in Fig. 5. Sign  $v_r$  is

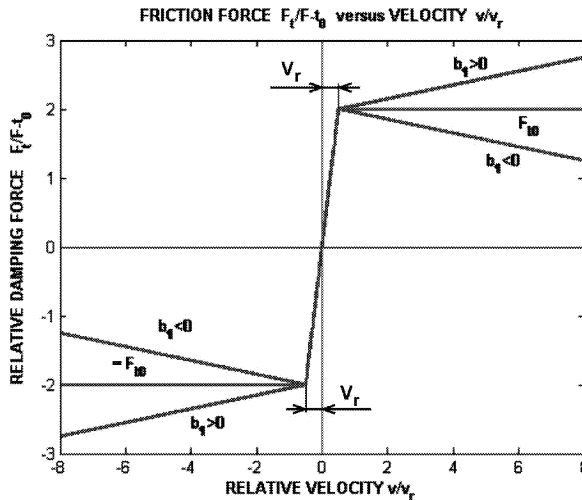


Fig.5

a velocity at which the micro-slip motion changes into full relative motion,  $F_{t0}$  is Coulomb friction force, proportional to the normal pressure  $F_{t0} = f F_N$ , where  $F_N$  varies with the centrifugal force.

This basic dry-friction model can be completed by further functions expressing the behaviour at higher relative velocities. For our purposes it is sufficient to use simple linear function so that the friction characteristic is described by equation:

$$F_t = F_{t0} \frac{v}{v_r} [1 - H(|v| - v_r)] + \left\{ F_{t0} \frac{v}{|v|} + b_1 [v - v_r \operatorname{sign}(v)] \right\} H(|v| - v_r), \quad (2)$$

where  $H$  is Heaviside function

$$H(x) = \begin{cases} 0 & \text{for } x \leq 0, \\ 1 & \text{for } x > 0 \end{cases}$$

and  $b_1$  expresses the increasing ( $b_1 > 0$ ) or decreasing ( $b_1 < 0$ ) friction force.

For numerical calculation of the disk motion it is suitable to replace the piecewise-linear function, assuming that  $q \approx q_0 \sin \omega t$ ,  $\dot{q} = v \approx q_0 \omega \cos \omega t = v_0 \cos \omega t$ , by equivalent linear damping function  $b_e(v_0) \dot{q}$  with the damping coefficient [6]

$$b_e(v_0) = \frac{1}{\pi v_0} \int_0^{2\pi} F_t(v_0 \cos \omega t) \cos \tau \, d\tau, \quad (3)$$

where  $v_0 = q_0 \omega$  is a velocity amplitude. For the basic Coulomb dry friction ( $b_1 = 0$ ), vibration  $v = v_0 \cos \tau$ ,  $\tau = \omega t$  reaches the value  $v = v_r$  at dimensionless time  $\tau_r$  when

$$v_r = v_0 \cos \tau_r. \quad (4)$$

Inserting function (2) for  $b_1 = 0$  into formula (3) gives:

$$b_0(v_0) = \frac{F_{t0}}{\pi v_0} \int_0^{2\pi} \left\{ \frac{v_0 \cos \tau}{v_r} [1 - H(|v_0 \cos \tau| - v_r)] + \frac{v_0 \cos \tau}{|v_0 \cos \tau|} H(|v_0 \cos \tau| - v_r) \right\} \cos \tau \, d\tau. \quad (5)$$

This integral should be solved in several parts of time intervals with a boundary  $\tau_r$ , which position is shown in Fig. 6. One period of motion is drawn there in relative values: relative velocity  $v(\tau)/v_r$  and dimensionless time  $\tau = \omega t$ .  $v_r$  is boundary velocity, at which the full slip motion passes into micro-slip motion, and  $\tau_r$  is corresponding dimensionless time.

Boundary time  $\tau_r$  is

$$\tau_r = \arccos \frac{v_r}{v_0}. \quad (6)$$

The equivalent damping coefficient  $b_e(v_0)$  for small micro-slip vibrations, when  $v_0 < v_r$ , is constant

$$b_e(v_0) = \frac{F_{t0}}{v_r}. \quad (7)$$

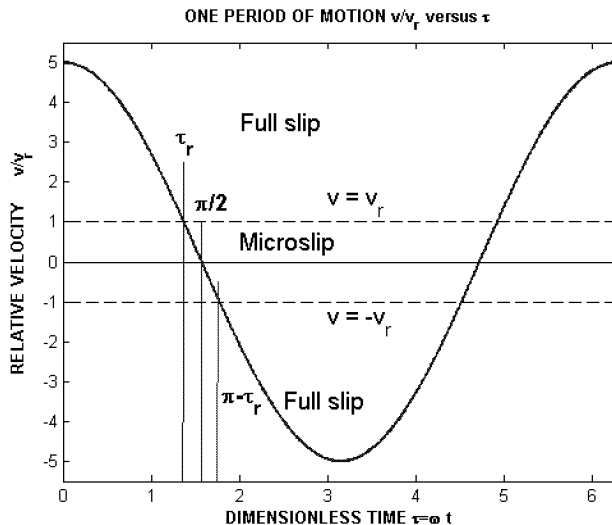


Fig.6

For higher amplitudes  $v_0$  of velocity is  $\cos \tau_r = v_r/v_0$  smaller than 1, boundary time  $\tau_r$  is real, smaller than  $\pi/2$  and equivalent linear damping coefficient is

$$\begin{aligned}
 b_e(v_0) &= \frac{F_{t0}}{\pi v_0} 4 \int_0^{\tau_r} \cos \tau \, d\tau + \frac{F_{t0}}{\pi v_r} 4 \int_{\tau_r}^{\pi/2} \cos^2 \tau \, d\tau = \\
 &= \frac{F_{t0}}{\pi v_r} 4 \left[ \frac{v_r}{v_0} \sin \tau_r + \frac{\pi}{4} - \frac{\tau_r}{2} - \frac{1}{2} \sin \tau_r \cos \tau_r \right] \pm b_1,
 \end{aligned} \tag{8}$$

where the linear damping coefficient  $\pm b_1$  is added.

After replacing boundary time  $\tau_r$  by relative velocity amplitude  $v_0/v_r$  (see (6)) we get

$$b_e(v_0) = \frac{F_{t0}}{\pi v_r} 2 \left[ \frac{\pi}{2} - \arccos\left(\frac{v_r}{v_0}\right) + \frac{v_r}{v_0} \sqrt{1 - \left(\frac{v_r}{v_0}\right)^2} \right] \pm b_1. \tag{9}$$

Graphical representation of this function is shown in Fig.7, where  $b_r = F_{t0}/v_r$  is the micro-slip gradient. After crossing boundary velocity  $v_r$ , the equivalent linear damping coefficient  $b_e(v_0)$  decreases roughly according to the hyperbolic law.

The limitation of equivalent linear damping coefficient  $b_e(v_0)$  corresponds to the real friction contact properties and is very useful also at numerical solution, as for classical Coulomb law  $b_e \rightarrow \infty$  for  $v_0 \rightarrow 0$ .

## 5. Vibration of stationary imperfect disk with nonlinear damping

Perfect circular disk vibrate by many modes, characterized by number  $n$  of nodal diameters (ND) and number  $l$  of nodal circles (NC). The forms of these modes belonging to one eigenfrequency  $\Omega_{(n,l)}$  can be described by

$$z_{(n,l)}(r, \varphi) = q_s f_l(r) \sin(n \varphi + \alpha_{(n,l)}) + q_c f_l(r) \cos(n \varphi + \alpha_{(n,l)}) \tag{10}$$

where  $q_s$ ,  $q_c$  are amplitudes of two orthogonal, sinus and cosines circumferential forms,  $f_l(r)$  express the form of deformation in radial direction. Roots  $r_l$  of equation  $f_l(r)$  as-

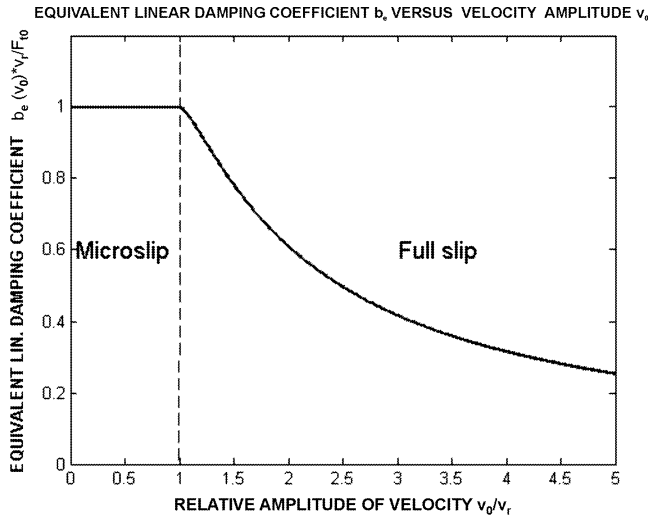


Fig.7

certain radii of nodal circle. Angle  $\alpha_{(n,l)}$  gives the position of nodal diameter at eigenfrequency  $\Omega_{(n,l)}$ . This angle is arbitrary at each mode being given by the initial conditions and distribution of external excitation.

Groups of damping heads added to a diameter at  $\varphi = 0$  transform the perfect disk into imperfect one. At small weight of damping heads, the modes of vibrations can be supposed unchanged and the equation (10) is valid as well, but the positions of nodal diameters are not arbitrary and both orthogonal forms have fixed nodal diameters at  $\alpha_{(n,l)} = 0$ . Sine-form has one nodal diameter passing through the position of added masses, while in cosine-form lie these masses on one antinodal diameter.

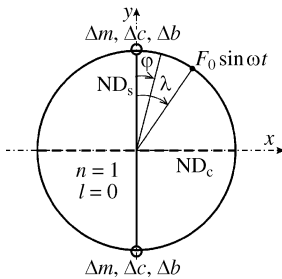


Fig.8

Let us suppose that an external harmonic transverse force  $F_0 \sin \omega t$  acts on the periphery of an imperfect disk in a point given by angle  $\lambda$  (Fig. 8). Disk is damped by dry friction elements. If the exciting frequency  $\omega$  is close to the split frequencies  $\Omega_{(n,l)s}$  and  $\Omega_{(n,l)c}$  we can neglect the influence of other nonresonant frequencies and the response can be describe only by these two predominate modes of vibrations.

Equations of motion are after dividing by reduced masses are :

$$\begin{aligned} \ddot{q}_s + \beta_s(\dot{q}_s) \dot{q}_s + \Omega_s^2 q_s &= K_s f(r) \sin n\varphi F_0 \sin \omega t \sin \lambda , \\ \ddot{q}_c + \beta_c \dot{q}_c + \Omega_c^2 q_c &= K_c f(r) \cos n\varphi F_0 \sin \omega t \cos \lambda , \end{aligned} \tag{11}$$

where

$$\begin{aligned} \beta_s(\dot{q}_s) &= \frac{b_{red} + 2 \Delta b(\dot{q}_s)}{m_{red}} , & \beta_c &= \frac{b_{red}}{m_{red} + 2 \Delta m} , \\ \Omega_s^2 &= \frac{c_{red}}{m_{red}} , & \Omega_c^2 &= \frac{c_{red} + 2 \Delta c_b}{m_{red} + 2 \Delta m} , \\ K_s &= \frac{K}{m_{red}} , & K_c &= \frac{K}{m_{red} + 2 \Delta m} . \end{aligned} \tag{12}$$

All these parameters are constant, with the exception of nonlinear damping  $\beta_s(\dot{q}_s)$ , where expression  $2 \Delta b(\dot{q}_s)/m_{red}$  is equivalent linear damping coefficient described by a function similar to (9), see Fig. 7.

Dynamic properties of such nonlinearly damped system are demonstrated on an example of imperfect disk excited in the frequency range including first eigenfrequency  $n = 1$ , which according to Table 1 is

$$f \in (40, 70) \text{ Hz} , \quad \omega \in (250, 450) \text{ s}^{-1} .$$

If the exciting force acts at the end of nodal diameter  $ND_c$  i.e.  $\lambda = n/2$  then only sine mode (frequency  $\Omega_{(1,0)s} = 370 \text{ s}^{-1}$ ) can arise.

Resonance curve of such case is shown in Fig. 9 where the damping coefficient is given by

$$\beta = \beta_0 + \alpha \frac{2}{\pi} \left[ \frac{\pi}{2} - \arccos \left( \frac{v_r}{v} \right) + \frac{v_r}{v} \sqrt{1 - \left( \frac{v_r}{v} \right)^2} \right] , \tag{13}$$

$\beta_0$  is damping of steel structure,  $\alpha$  denotes the intensity of friction force, proportional to the centrifugal force.

Curves in Fig. 9 were calculated for the force amplitude  $K_s f(r) F_0 = 100$  and for different friction force characterize by parameter  $\alpha = 20, 50, 100$ .

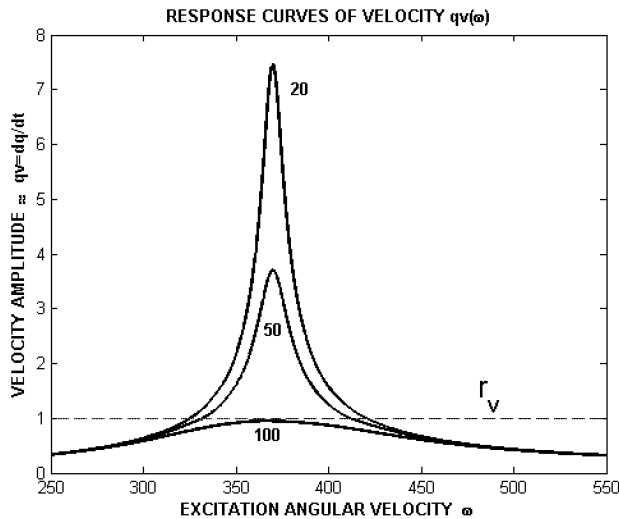


Fig.9

## 6. Rotating imperfect disk with friction dampers

Dynamical properties of disk rotating with angular velocity  $v$  are influenced by increasing stiffness due to the centrifugal forces. Revolutions of experimental equipment in IT AS CR are comparatively low and therefore this influence can be neglected in following analysis.

May a harmonic force  $F_0 \sin \omega t$  acts in fixed space position ( $\varphi_a = 0$ ) on the rotating disk. In the coordinate system  $r, \varphi$  related with rotating disk, this force moves in the negative direction  $\varphi$  and excites all modes of vibration.

Provided the initial condition is  $\varphi = \varphi_a = 0$  in  $t = 0$ , then the position of force on the rotating disk is  $\lambda = -vt$ . The dynamic properties of rotating disk excited by an in-space-standing force can be investigated by the same equations (2,3), but with a substitution  $\lambda = -vt$ :

$$\begin{aligned}\ddot{q}_s + \beta_s(\dot{q}_s) \dot{q}_s + \Omega_s^2 q_s &= \frac{K f(r) F_0}{m_r} \sin \varphi \sin \omega t \sin(-vt) , \\ \ddot{q}_c + \beta_c \dot{q}_c + \Omega_c^2 q_c &= \frac{K f(r) F_0}{m_r} \cos \varphi \sin \omega t \cos(-vt) .\end{aligned}\quad (14)$$

It is convenient to replace the products of time functions on the right sides of these equations by sums of harmonic functions

$$\begin{aligned}\sin \omega t \sin(-vt) &= \frac{1}{2} [\cos(\omega + v)t - \cos(\omega - v)t] , \\ \sin \omega t \cos(-vt) &= \frac{1}{2} [\sin(\omega + v)t + \sin(\omega - v)t] .\end{aligned}\quad (15)$$

Using decomposition (15) and a new designation  $Q = K f(r) F_0 / (2 m_r)$ , the solution of (14) can be written in a following form:

$$\begin{aligned}q_{s0} &= \frac{Q \sin \varphi \cos[(\omega + v)t - \Psi_{s1}]}{\sqrt{[\Omega_s^2 - (\omega + v)^2]^2 + \beta_s^2(\dot{q}_{s0}) (\omega + v)^2}} - \frac{Q \sin \varphi \cos[(\omega - v)t - \Psi_{s2}]}{\sqrt{[\Omega_s^2 - (\omega - v)^2]^2 + \beta_s^2(\dot{q}_{s0}) (\omega - v)^2}} , \\ q_{c0} &= \frac{Q \cos \varphi \sin[(\omega + v)t - \Psi_{c1}]}{\sqrt{[\Omega_c^2 - (\omega + v)^2]^2 + \beta_c^2 (\omega + v)^2}} + \frac{Q \cos \varphi \sin[(\omega - v)t - \Psi_{c2}]}{\sqrt{[\Omega_c^2 - (\omega - v)^2]^2 + \beta_c^2 (\omega - v)^2}} , \\ q(\varphi, t) &= q_s + q_c .\end{aligned}\quad (16)$$

The phase angles are

$$\begin{aligned}\Psi_{s1} &= \arctan \frac{\beta_s(\dot{q}_{s0}) (\omega + v)}{\Omega_c^2 - (\omega + v)^2} , & \Psi_{s2} &= \arctan \frac{\beta_s(\dot{q}_{s0}) (\omega - v)}{\Omega_c^2 - (\omega - v)^2} , \\ \Psi_{c1} &= \arctan \frac{\beta_c (\omega + v)}{\Omega_c^2 - (\omega + v)^2} , & \Psi_{c2} &= \arctan \frac{\beta_c (\omega - v)}{\Omega_c^2 - (\omega - v)^2} ,\end{aligned}\quad (17)$$

where  $\dot{q}_{s0}$  is amplitude of velocity of the sine mode in the resonance zone around the eigenfrequency  $\Omega_s$ .

The denominators of fractions in (16) reach their lowest magnitudes at zero values of first great brackets – at excitation frequencies:

$$\omega = \Omega_s - v , \quad \omega = \Omega_s + v , \quad \omega = \Omega_c - v , \quad \omega = \Omega_c + v , \quad (18)$$

where the resonance peaks in response curves  $q(\omega)$  at constant disk revolutions occur.

## 7. Response curves of rotating imperfect disk with friction dampers

The total response of rotating disk on a standing single point harmonic excitation consists of four harmonic components (16,17) with different frequencies, amplitudes, phase angles being also dependent on position on disk determined by angle  $\varphi$ . The calculation and also graphical demonstration of this response is difficult.

However, the steel bladed disks are only lightly damped and resonance peaks are very sharp and so the separate solving of single resonances is acceptable. Sum of these amplitudes

gives the maximal possible amplitudes at given frequency  $\omega$ . Let us according to measurement on the experimental bladed disk IT choose the lowest eigenfrequency  $\Omega_s = 260$  rad/s,  $\Omega_c = 380$  rad/s. If angular velocity of rotating disc is  $v = 30$  rad/s then resonances are at  $\omega = 230, 290, 350$  and  $410$  rad/s.

Response of rotating disk on the standing harmonic excitation is shown in Fig. 10, where the amplitude of velocity  $\dot{q}_0 = (dq/dt)_{\max} = q_0 \omega$  calculated from equation (16) for generalized force  $Q = K f(r) F_0 / (2 m_r) = 50$  is plotted versus frequency  $\omega$ . Damping coefficient for the cosine mode is constant  $\beta_c = 2$  and therefore for sine mode holds:

$$\beta_s(\dot{q}_0) = 2 + \alpha \frac{2}{\pi} \left[ \frac{\pi}{2} - \arccos\left(\frac{v_r}{\dot{q}_0}\right) + \frac{v_r}{\dot{q}_0} \sqrt{1 - \left(\frac{v_r}{\dot{q}_0}\right)^2} \right] H(|\dot{q}_0| - v_r) + \alpha \frac{\dot{q}_0}{v_r} [1 - H(|\dot{q}_0| - v_r)] . \tag{19}$$

Parameter  $\alpha$  representing a level of friction damping is variable. In Fig. 10 there are drawn three alternatives for  $\alpha = 10, 20, 40$ . Friction dampers change the sine modes and decrease the split resonances, but on the cosine modes they have no influence.

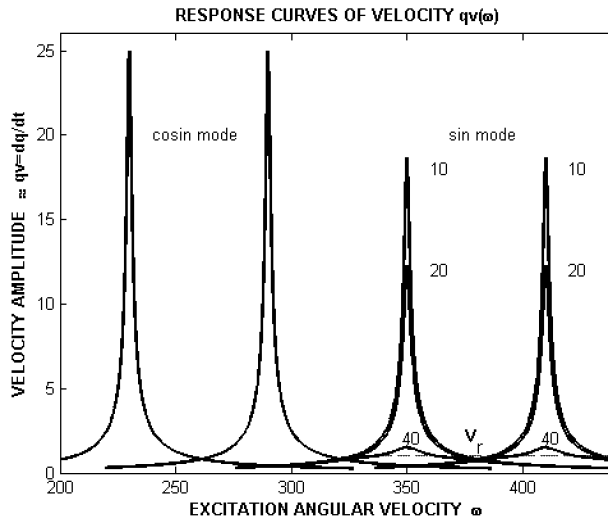


Fig.10

### 8. Non-proportional damping

Equations (11) or (14), were compiled at the assumption, that the additional damping  $\Delta b$  influences the modes of vibration in the similar way as  $b_{red}$ , i.e. as uniformly distributed damping within all elements of investigated disk. This assumption causes that the height of resonant peaks continuously decreases for increasing coefficient  $\alpha$  of friction force as it can be seen in Fig. 9 and 10. However this feature is in contradiction with the real behavior of friction dampers fixed only on limited number of blades. Indeed the

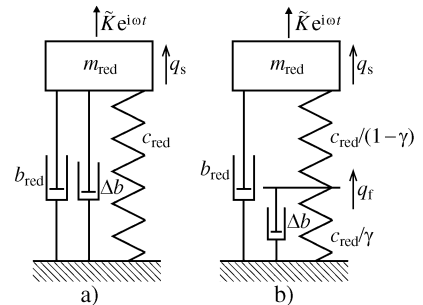


Fig.11

very high friction does not allow any relative motion, and consequently the stiffness of corresponding part of disk increases, but the additional damping approaches to zero. Therefore there exists some optimum damping, where the friction dampers are the most effective.

For modeling of such properties, the up to now applied vibrating system outlined in Fig. 11a should be replaced by system in Fig. 11b, where friction damper influences only  $\gamma$  part of vibrating system – elastic disk.

Equations of motion of disk in a frequency range of first split eigenfrequency instead of (11) are as follows:

$$\begin{aligned} m_{\text{red}} \ddot{q}_s + b_{\text{red}} \dot{q}_s + \frac{c_{\text{red}}}{1-\gamma} (q_s - q_f) &= K f(r) F_0 \sin \varphi \sin \omega t \sin \lambda, \\ (q_s - q_f) \frac{c_{\text{red}}}{1-\gamma} &= \frac{c_{\text{red}}}{\gamma q_f} + \alpha b_e (\dot{q}_{f0}) \dot{q}_f, \\ (m_{\text{red}} + 2 \Delta m) \ddot{q}_c + b_{\text{red}} \dot{q}_c + (c_{\text{red}} + 2 \Delta c) q_c &= K f(r) F_0 \cos \varphi \sin \omega t \cos \lambda, \end{aligned} \quad (20)$$

where  $\dot{q}_{f0}$  is the amplitude of velocity  $\dot{q}_f$  in the upper-point of dry friction element (see Fig. 11). For simplicity let us suppose that the additional damping is linear  $b_e(\dot{q}_{f0}) = b_e$ . Introducing following abbreviations:

$$\beta_0 = \frac{b_{\text{red}}}{m_{\text{red}}}, \quad \Omega^2 = \frac{c_{\text{red}}}{m_{\text{red}}}, \quad \tilde{K} = \frac{K f(r) F_0}{m_{\text{red}}} \sin \varphi \sin \lambda, \quad bet = \frac{b_e}{c_{\text{red}}}$$

and replacing  $\sin \omega t$  by  $e^{i\omega t}$ , the first two equations (20) are

$$\begin{aligned} \ddot{q}_s + \beta_0 \dot{q}_s + \frac{\Omega^2}{1-\gamma} (q_s - q_f) &= \tilde{K} e^{i\omega t}, \\ q_s &= \frac{q_f}{\gamma} + \alpha bet \dot{q}_f \frac{1-\gamma}{c_{\text{red}}}. \end{aligned} \quad (21)$$

Particular solution is  $q_s = A e^{i\omega t}$ ,  $q_f = B e^{i\omega t}$  where complex amplitudes  $A, B$  satisfy equation

$$\begin{bmatrix} \frac{\Omega^2}{1-\gamma} - \omega^2 + i\omega \beta_0 & -\frac{\Omega^2}{1-\gamma} \\ 1 & -\frac{1}{\gamma} - i\omega \alpha bet \frac{1-\gamma}{c_{\text{red}}} \end{bmatrix} \begin{bmatrix} A \\ B \end{bmatrix} = \begin{bmatrix} \tilde{K} \\ 0 \end{bmatrix}. \quad (22)$$

Determinant of the system matrix reads:

$$D = \frac{\omega^2 - \Omega^2}{\gamma} + \omega^2 \alpha \beta_0 bet \frac{1-\gamma}{c_{\text{red}}} - i\omega \left[ \frac{\beta_0}{\gamma} + \alpha bet \left( \frac{\Omega^2}{1-\gamma} - \omega^2 \right) \frac{1-\gamma}{c_{\text{red}}} \right] \quad (23)$$

and hence amplitudes

$$\begin{aligned} A &= \left( -\frac{1}{\gamma} - i\omega \alpha bet \frac{1-\gamma}{c_{\text{red}}} \right) \frac{\tilde{K}}{D}, \\ B &= -\frac{\tilde{K}}{D}, \\ \dot{q}_{f0} &= \omega |B| = \omega \frac{\tilde{K}}{|D|}. \end{aligned} \quad (24)$$

Squaring the last equation (24), we obtain after a rearrangement

$$\left[ \frac{\omega^2 - \Omega^2}{\gamma} + \omega^2 \alpha \beta_0 \text{bet} \frac{1 - \gamma}{c_{\text{red}}} \right]^2 + \omega^2 \left[ \frac{\beta_0}{\gamma} + \alpha \beta_0 \text{bet} \left( \frac{\Omega^2}{1 - \gamma} - \omega^2 \right) \frac{1 - \gamma}{c_{\text{red}}} \right]^2 - \frac{\omega^2 \tilde{K}^2}{\dot{q}_{f0}^2} = 0 . \tag{25}$$

Eq.(25) provides for given system parameters  $\Omega$ ,  $\gamma$ ,  $\alpha$ ,  $\beta_0$ ,  $\tilde{K}$  the dependence between frequency  $\omega$  and velocity amplitude  $\dot{q}_{f0}$ . For better convenience, the above relationship in a polynomial form should be written :

$$a \omega^6 + b \omega^4 + c \omega^2 + d = 0 , \tag{26}$$

where

$$\begin{aligned} a &= \left( \alpha \text{bet} \frac{1 - \gamma}{c_{\text{red}}} \right)^2 , \\ b &= \left( \frac{1}{\gamma} + \beta_0 \alpha \text{bet} \right)^2 - 2 \alpha \text{bet} \frac{1 - \gamma}{c_{\text{red}}} \left( \frac{\beta_0}{\gamma} + \frac{\Omega^2}{1 - \gamma} \alpha \text{bet} \frac{1 - \gamma}{c_{\text{red}}} \right) , \\ c &= \left( \frac{\beta_0}{\gamma} + \frac{\Omega^2}{1 - \gamma} \alpha \text{bet} \frac{1 - \gamma}{c_{\text{red}}} \right)^2 - \frac{2 \Omega^2}{\gamma} \left( \frac{1}{\gamma} + \beta_0 \alpha \text{bet} \frac{1 - \gamma}{c_{\text{red}}} \right) - \frac{\tilde{K}^2}{\dot{q}_{f0}^2} , \\ d &= \frac{\Omega^4}{\gamma^2} . \end{aligned} \tag{26a}$$

Difference between response curves of systems drawn in Fig. 11a and 11b can be shown for linear additional damping  $\Delta b \approx \alpha b_e \dot{q}_f$  where  $b_e$  is constant (see Fig. 12). Other system parameters let be :

$$\begin{aligned} m_{\text{red}} &= 1 \text{ kg} , \quad c_{\text{red}} = 10^4 \text{ kg s}^{-2} , \quad b_{\text{red}} = 10 \text{ kg s}^{-1} , \\ \tilde{K} &= K f(r) F_0 \sin \lambda = 10^4 \text{ N} , \quad \Delta b = \alpha b_e = \alpha 100 \text{ kg s}^{-1} . \end{aligned}$$

Let the damping parameter  $\alpha$  varies in a large range from  $\alpha = 0$  to  $\alpha = 500$ . Parameter  $\gamma = 0.2$  of partial damping corresponds to the system in Fig. 11b, value  $\gamma = 1$  corresponds to the system in Fig. 11a.

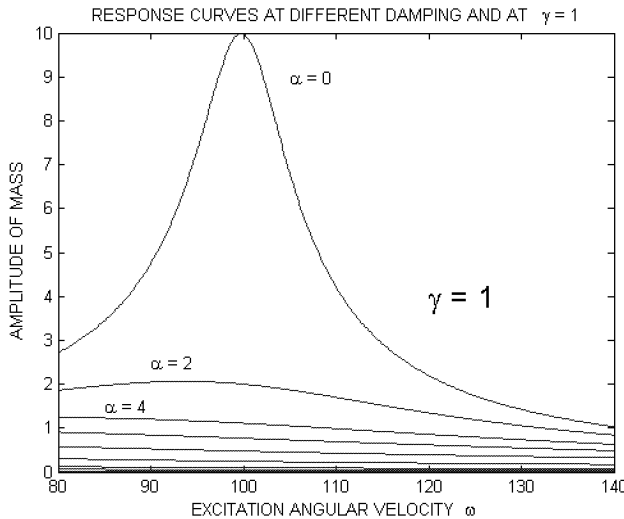


Fig.12

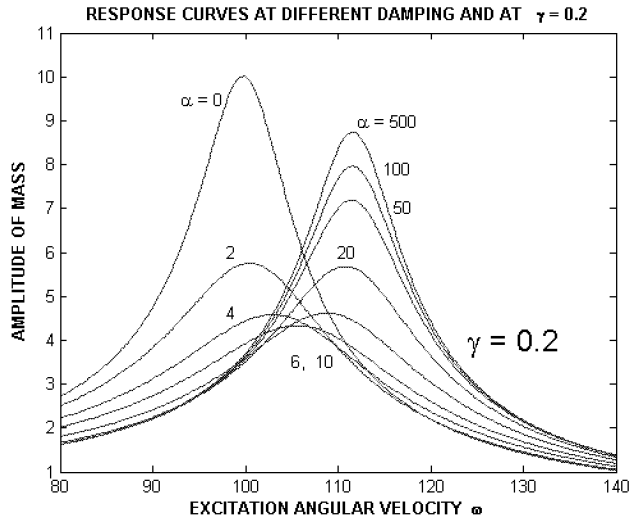


Fig.13

From the responses of motion  $q_s$  of mass  $m_{red}$  on the harmonic excitation  $\tilde{K} e^{i\omega t}$  for increasing damping parameter in Fig. 12, it is evident that the greater is damping at  $\gamma = 1$ , the lower is resonance amplitude.

Another situation occur when the damping is distributed non-proportional to the elastic property and acts only on a part of elastic spring. The set of response curves for  $\gamma = 0.2$  and  $\alpha = 0, 2, 4, 10, 20, 50, 100$  and  $500$  is drawn in Fig. 13.

It is evident that in the amplitudes for values  $\alpha \in (0, 5)$  decrease with increasing damping, but an optimal system damping exists (approximately for  $\alpha = 6$  thick line), where the resonance peak is lowest. Further increase of damping ( $\alpha > 6$ ) causes again the rise of resonance amplitudes, related also with increase of resonance frequency.

## 9. Conclusion

Up to now, the research developing the theoretical support of experimental investigation of rotating model of bladed disk which has been carried out in Institute of Thermomechanics ASCR with the aim to investigate the influence of elastic, mass and damping imperfections on the dynamic behavior of turbine disks was based on linear model. The used dry friction damping elements in the added heads have strong nonlinear characteristics, which considerable influence the vibrations properties of the whole bladed disk.

Analysis of dynamic response of both standing and rotating imperfect disk excited by an external in space fixed harmonic transversal force shows great sensitivity of resonance peak's height on the level of pressure in the friction contact area expressed in presented analysis by a parameter  $\alpha$ . This influence is find out at the resonance peaks corresponding to the sine mode with the nodal diameter passing through imperfections originating from added damper heads, while the other split resonance peaks corresponding to the cosine mode with the perpendicular nodal diameter didn't prove changes at all.

Non-proportional distribution of damping induces an existence of an optimal damping, at which the resonance amplitude is minimum. The further increase of damping heightens

amplitude of vibration. The entire system is getting stiffer and corresponding resonance peak shifts to the higher frequency.

Analysis using equivalent linearization method of solution was in this article limited on the lowest modes with one nodal diameter without any nodal circle. However, the developed method of solution can be applied on every higher, more complicated modes of vibrations.

### Acknowledgement

This work has been elaborated in a frame work of the grant project GA CR 101/09/1166 ‘Research of dynamic behaviour and optimisation of complex rotating system with non-linear couplings and high damping materials’.

### References

- [1] Tobias S.A., Arnold R.N.: The Influence of Dynamical Imperfection on the Vibration of Rotating Disks, Proc. Inst. Mech. Engrs, 171, Edinburgh, p. 669–690, (1957)
- [2] Torii T., Yasuda K.: Nonlinear Oscillation of a Rotating Disk Subject to a Transverse Load at a Space-fixed Point, in: X. World Cong. on the Theory of Machine and Mechanisms (T. Leinonen, ed.), Oulu, Finland, p. 1752–1757, (1999)
- [3] Yan Li-Tang, Li Qi-Han: Investigation of Travelling Wave Vibration for Bladed Disk in Turbomachinery, in: Proc. 3rd Int. Conf. on Rotordynamics – IFToMM (Lalanne, M., ed.), Lyon, p. 133–135, (1990)
- [4] Pešek L. et al.: Dynamics of Rotating Blade Disk Identical by Magneto-Kinematic Measuring System, in: Proc. ISMA 2008, (Sas P., Bergen B., eds), Katholieke Univ. Leuven, p. 1097–1111, (2008)
- [5] Pešek L. et al.: Development of Excitation and measurement for identification of rotating blade disk, in: Proc. SIRM 2009, Int. Conf. On Vibrations in Rotating Machines, TU Vienna, ID-8, p. 1–10, (2009)
- [6] Brepta R., Půst L., Turek F.: Mechanické kmitání, Technický průvodce 71, Sobotáles, Praha, (1994)
- [7] Půst L., Pešek L.: Traveling Waves in Rotational Machines, in: Proc. Engineering Mechanics 2009, (Náprstek J., Fischer C., eds.) ITAM ASCR, Prague, CD ROM, p. 1065–1078, (2009)
- [8] Půst L., Pešek L.: Traveling Waves in circular Disk with Imperfections, in: 10. Conf. on Dynamical Systems – Theory and Applications, DESTA 2009, Lodž, Vol. I, pp. 345–352, (2009)
- [9] Půst L., Pešek L.: Nonlinear damping in rotating disk, in: Conf. Dynamics of Machines 2010, IT ASCR, Prague, pp. 63–72, (2010)

*Received in editor's office:* March 23, 2010

*Approved for publishing:* June 1, 2010

*Note:* This paper is an extended version of the contribution presented at the national colloquium with international participation *Dynamics of Machines 2010* in Prague.